

## Supplementary Materials

### A facile and eco-friendly hydrothermal synthesis of high tetragonal barium titanate with uniform and controllable particle size

Tingting Wang <sup>1</sup>, Xiaoxiao Pang <sup>1</sup>, Bin Liu <sup>1</sup>, Jie Liu <sup>1</sup>, Jing Shen <sup>2</sup> and Cheng Zhong <sup>1,3,\*</sup>

<sup>1</sup> Key Laboratory of Advanced Ceramics and Machining Technology (Ministry of Education), School of Materials Science and Engineering, Tianjin University, Tianjin 300072, China; wtt@tju.edu.cn (T.W.); xiaoxiao\_pang17@163.com (X.P.); arthurlou@tju.edu.cn (B.L.); jieliu0109@tju.edu.cn (J.L.).

<sup>2</sup> Chongqing Newcent New Materials Co., Ltd. Chongqing 401147, China;  
shenjing@chinanewcent.com (J.S.).

<sup>3</sup> Joint School of National University of Singapore and Tianjin University, International Campus of Tianjin University, Binhai New City, Fuzhou 350207, China.

\* Correspondence: cheng.zhong@tju.edu.cn

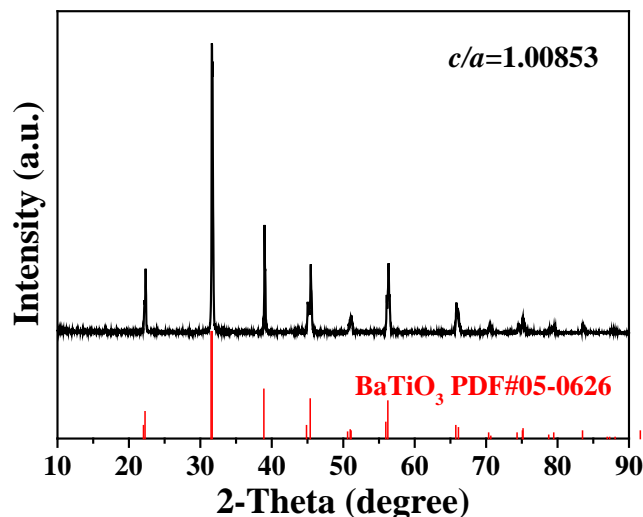


**Figure S1.** XRD pattern of BT powders. The hydrothermal solvent consists of 30 mL of water, 10 mL of ethanol and 10 mL of ammonia solution (3 : 1 : 1).

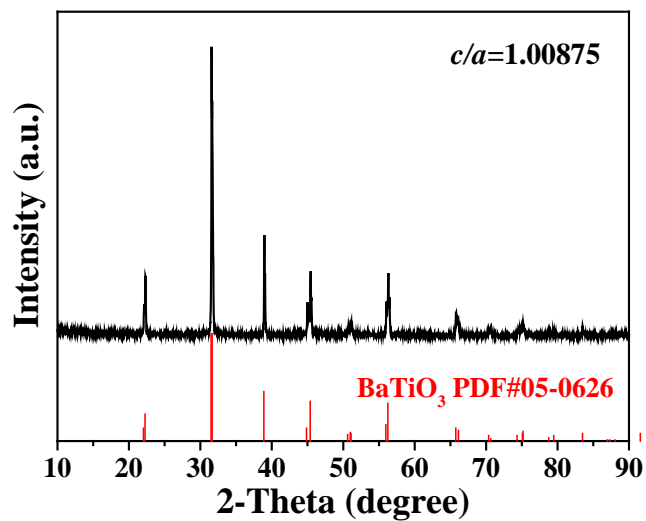


**Figure S2.** XRD pattern of BT powders. The hydrothermal solvent consists of 25 mL of water, 15 mL of ethanol and 10 mL of ammonia solution (5 : 3 : 2).

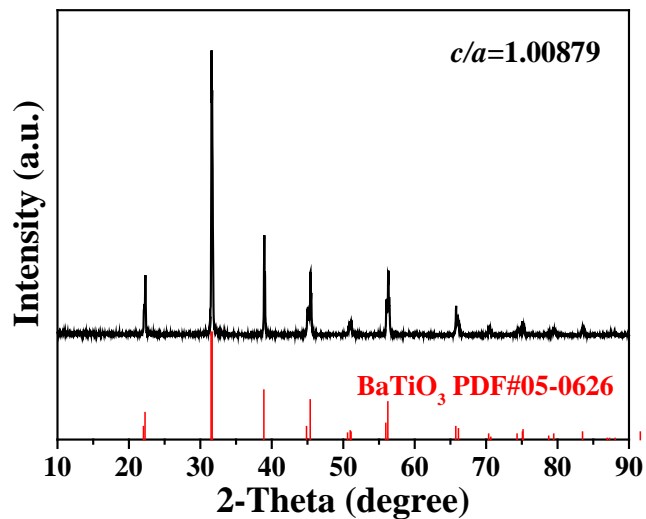


**Figure S3.** XRD pattern of BT powders. The hydrothermal solvent consists of 15 mL of water, 25 mL of ethanol and 10 mL of ammonia solution (3 : 5 : 2).

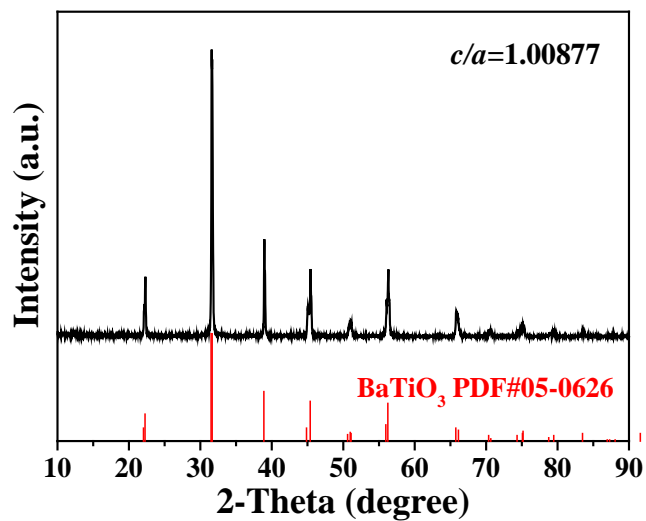


**Figure S4.** XRD pattern of BT powders. The hydrothermal solvent consists of 10 mL of water, 30 mL of ethanol and 10 mL of ammonia solution (1 : 3 : 1).

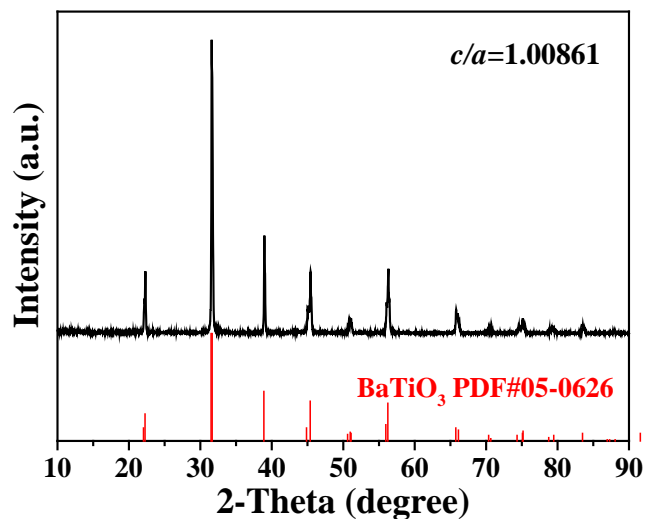


**Figure S5.** XRD pattern of BT powders. The hydrothermal solvent consists of 5 mL of water, 35 mL of ethanol and 10 mL of ammonia solution (1 : 7 : 2).

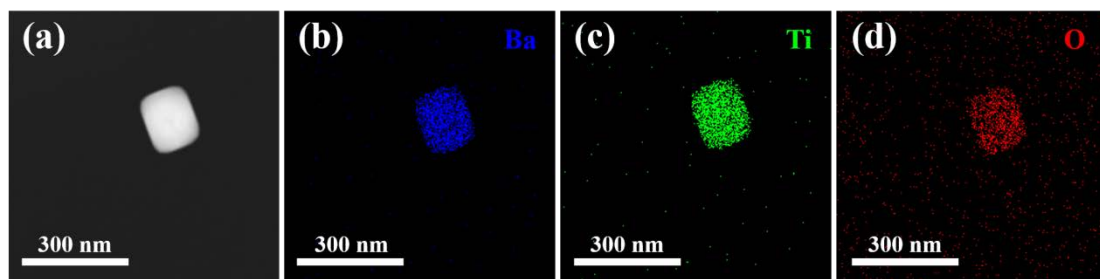


**Figure S6.** (a) STEM image and (b-d) EDS elements mapping of BT-160 sample.

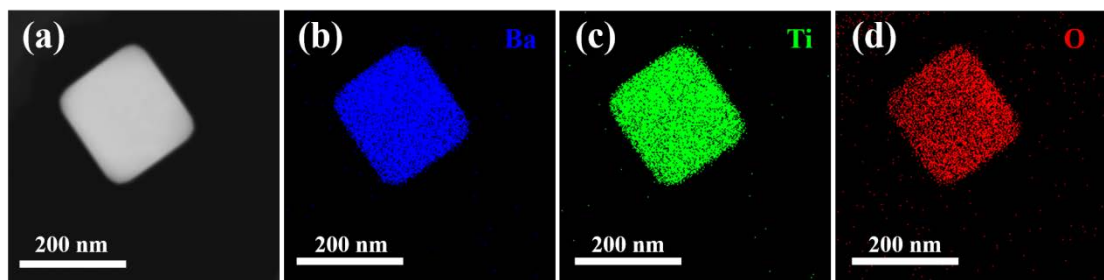


**Figure S7.** (a) STEM image and (b–d) EDS elements mapping of BT-220 sample.

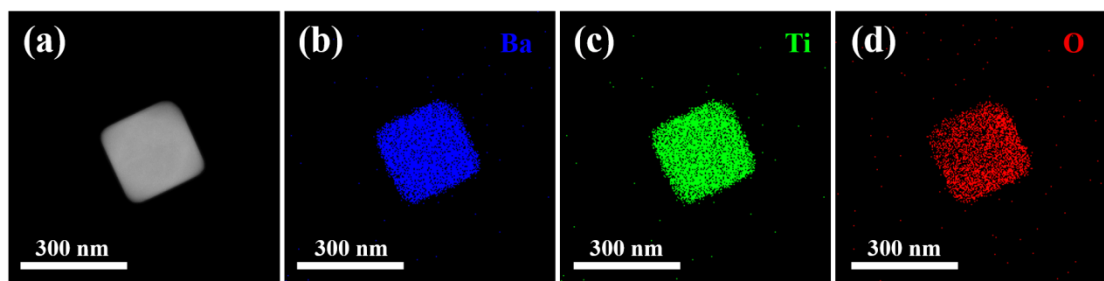


**Figure S8.** (a) STEM image and (b–d) EDS elements mapping of BT-250 sample.

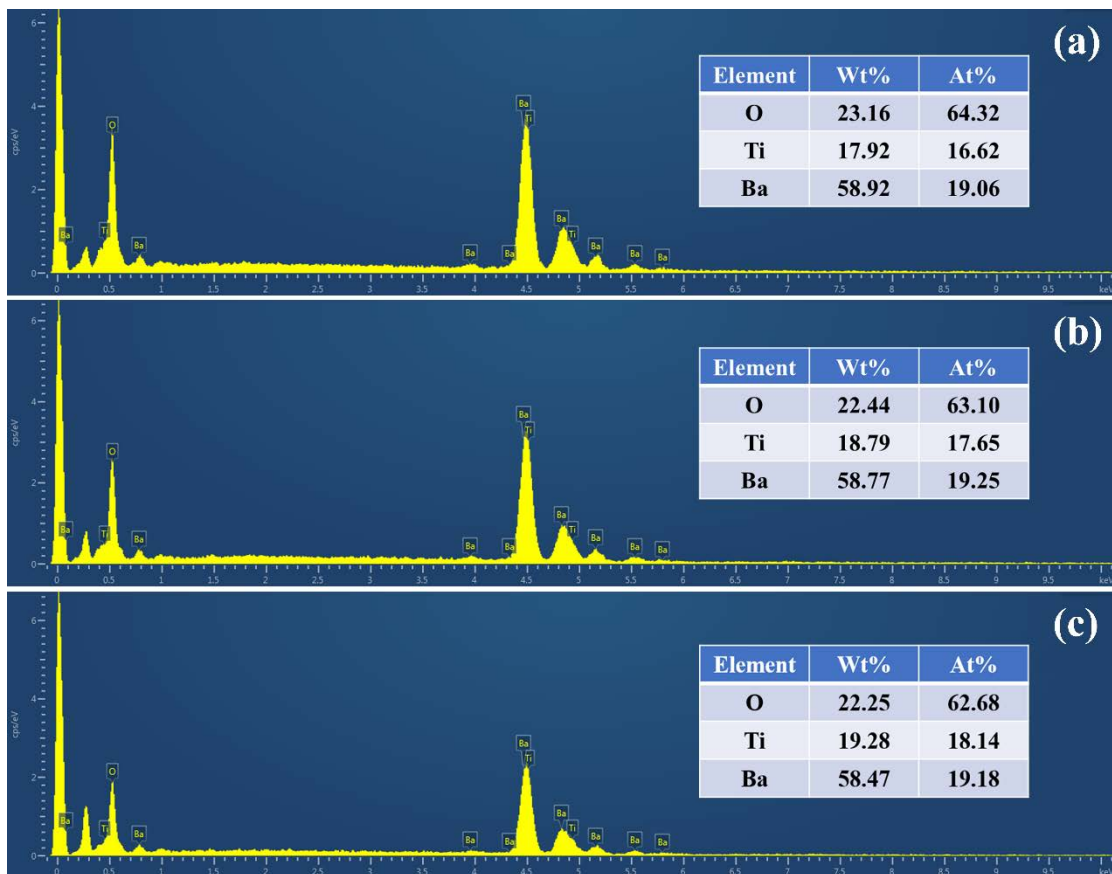


**Figure S9.** EDS results of (a) BT-160, (b) BT-220 and (c) BT-250 samples.

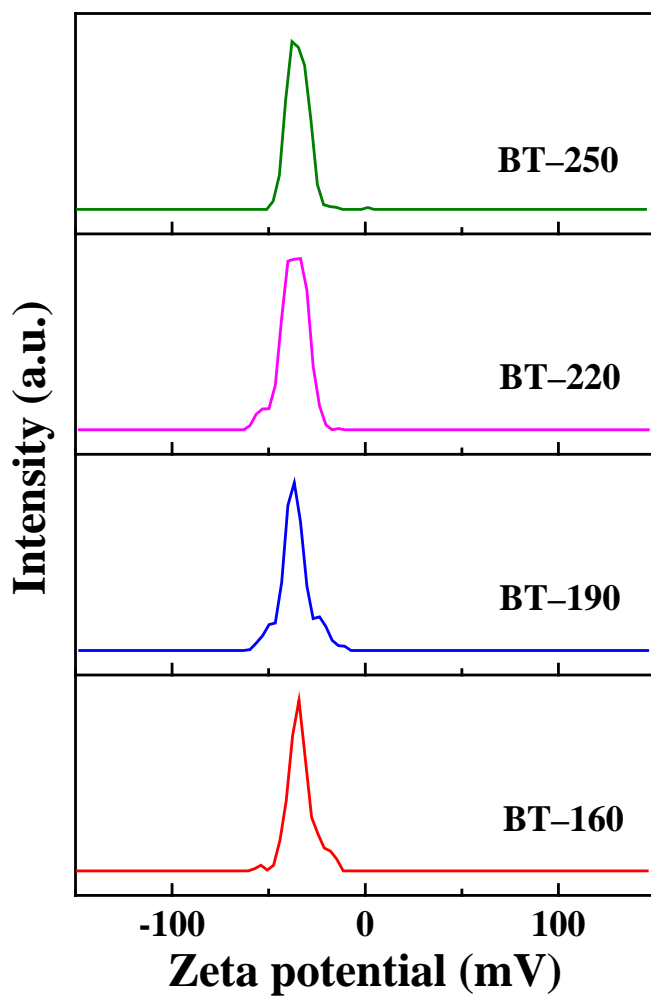


Figure S10. Zeta potential curves of four BT powders.



Figure S11. Photographs of (a) about 28 g of BT-190 product and (b) BT powders.

**Table S1** Specific values of the lattice parameters  $a$ ,  $c$  and their  $c/a$  ratios for four BT powders.

Samples	BT-160	BT-190	BT-220	BT-250
$a$	3.99292	3.99430	3.99400	3.99317
$c$	4.02874	4.03093	4.03091	4.03024
$c/a$	1.00897	1.00917	1.00924	1.00928

**Table S2** The ratios between tetragonal and cubic phases of four BT powders.

Samples	BT-160	BT-190	BT-220	BT-250
Tetragonal phase	89.8%	91.3%	92.3%	92.9%
Cubic phase	10.2%	8.7%	7.7%	7.1%

**Table S3.** Zeta potentials of four BT powders.

Samples	BT-160	BT-190	BT-220	BT-250
Zeta potential (mV)	-33.6	-36.1	-37.0	-34.9

**Table S4** Comparison of dual regulations of tetragonality and particle size prepared by the hydrothermal method.

Raw materials	$c/a$	particle size (nm)	Ref.
TiO <sub>2</sub> and Ba(OH) <sub>2</sub> ·8H <sub>2</sub> O	1.00897–1.00924	160–250	This work
TiO <sub>2</sub> and BaCl <sub>2</sub>	1.001–1.007	21–512	[1]
Ti(O <sup>i</sup> Pr) <sub>4</sub> and Ba(CH <sub>3</sub> COO) <sub>2</sub>	1.0063–1.0075	117–162	[2]
Ti(OC <sub>4</sub> H <sub>9</sub> ) <sub>4</sub> and Ba(OH) <sub>2</sub> ·H <sub>2</sub> O	1.0028–1.0073	96.1	[3]
TiO <sub>2</sub> and Ba(OH) <sub>2</sub> ·8H <sub>2</sub> O	1.000–1.007	69.8–119.0	[4]
(Ti(OC <sub>4</sub> H <sub>9</sub> ) <sub>4</sub> and Ba(OH) <sub>2</sub> ·8H <sub>2</sub> O	–	57–75	[5]
TiO <sub>2</sub> and Ba(OH) <sub>2</sub> ·8H <sub>2</sub> O	1.006–1.008	90–120	[6]
TiCl <sub>4</sub> and BaCl <sub>2</sub> ·2H <sub>2</sub> O	1.0001–1.0061	47–83	[7]
Ti[OC <sub>4</sub> H <sub>9</sub> ] <sub>4</sub> and Ba(CH <sub>3</sub> COO) <sub>2</sub>	1.0056–1.0076	85.18–112.12	[8]

## References

- Yan, Y.; Xia, H.; Fu, Y.; Xu, Z.; Ni, Q.-Q. Controlled Hydrothermal Synthesis of Different Sizes of BaTiO<sub>3</sub> Nano-Particles for Microwave Absorption. *Mater. Res. Express* **2020**, *6*, 1250i3. <https://doi.org/10.1088/2053-1591/ab6daf>
- Zamperlin, N.; Ceccato, R.; Fontana, M.; Pegoretti, A.; Chiappini, A.; Dire, S. Effect of Hydrothermal Treatment and Doping on the Microstructural Features of Sol-Gel Derived BaTiO<sub>3</sub>

- Nanoparticles. *Materials* **2021**, *14*, 4345. <https://doi.org/10.3390/ma14154345>
- 3 Meng, H.; Chen, Z.; Lu, Z.; Wang, X.; Fu, X. Hydrothermal Synthesis of Tetragonal Barium Titanate Nanopowders under Moderate Conditions. *Process. Appl. Ceram.* **2021**, *15*, 179–183. <https://doi.org/10.2298/pac2102179m>
  - 4 Hayashi, H.; Ebina, T. Effect of Hydrothermal Temperature on the Tetragonality of BaTiO<sub>3</sub> Nanoparticles and in-Situ Raman Spectroscopy under Tetragonal-Cubic Transformation. *J. Ceram. Soc. Jpn.* **2018**, *126*, 214–220. <https://doi.org/10.2109/jcersj2.17125>
  - 5 Chen, H.; Wang, J.; Yin, X.; Xing, C.; Li, J.; Qiao, H.; Shi, F. Hydrothermal Synthesis of BaTiO<sub>3</sub> Nanoparticles and Role of Pva Concentration in Preparation. *Mater. Res. Express* **2019**, *6*, 055028. <https://doi.org/10.1088/2053-1591/ab0520>
  - 6 Habib, A.; Stelzer, N.; Angerer, P.; Haubner, R. Effect of Temperature and Time on Solvothermal Synthesis of Tetragonal BaTiO<sub>3</sub>. *Bull. Mater. Sci.* **2011**, *34*, 19–23. <https://doi.org/10.1007/s12034-011-0043-2>
  - 7 Li, J.; Inukai, K.; Tsuruta, A.; Takahashi, Y.; Shin, W. Synthesis of Highly Disperse Tetragonal BaTiO<sub>3</sub> Nanoparticles with Core-Shell by a Hydrothermal Method. *J. Asian. Ceram. Soc.* **2018**, *5*, 444–451. <https://doi.org/10.1016/j.jascer.2017.09.006>
  - 8 Huang, Y.A.; Lu, B.; Li, D.D.; Tang, Z.H.; Yao, Y.B.; Tao, T.; Liang, B.; Lu, S.G. Control of Tetragonality Via Dehydroxylation of BaTiO<sub>3</sub> Ultrafine Powders. *Ceram. Int.* **2017**, *43*, 16462–16466. <https://doi.org/10.1016/j.ceramint.2017.09.027>